indicator is negligibly small. In the poorly buffered solutions under consideration this is not precisely true and the amount of perchloric acid reacting with the indicator must be taken into account. Defining p according to eq. 9a and b as the molarity of the base added to the pure salt solution, eq. 9b follows.

$$p = C_{BHClO_4} + C_B = C_B\,(C_{BHClO_4}/C_B + 1) \quad (9a)$$

$$C_B = b + C_{HClO_4} + [IHClO_4] \quad (9b)$$

Eliminating C_B by combining eq. 9a and 9b and substituting into the result $C_{HClO_4} = R/K_f^{IHClO_4}$ and C_{BHClO_4}/C_B as obtained from eq. 7c yields eq. 9c. Since $[IHClO_4] = (C_I)_t R/(R + 1)$

$$p = \left[\frac{K_f^{BHClO_4}}{K_f^{IHClO_4}} R + 1\right]\left[b + \frac{R}{K_f^{IHClO_4}} + [IHClO_4]\right] \quad (9c)$$

the quadratic expression is R, eq. 9d results. In the immediate vicinity of the equivalence point $K_f^{BHClO_4}/K_f^{IHClO_4}$ R is much larger than one, allowing eq. 9d to be simplified to eq. 9e which becomes eq. 9f in a pure salt solution

$$p = \left[\frac{K_f^{BHClO_4}}{K_f^{IHClO_4}} R + 1\right]\left[b + \frac{R}{K_f^{IHClO_4}} + \frac{(C_I)_t R}{R + 1}\right] \quad (9d)$$

$$p = R^2 \frac{K_f^{BHClO_4}}{K_f^{IHClO_4}}\left[\frac{b}{R} + \frac{1}{K_f^{IHClO_4}} + \frac{(C_I)_t}{R + 1}\right] \quad (9e)$$

$$p = R^2 \frac{K_f^{BHClO_4}}{K_f^{IHClO_4}}\left[\frac{1}{K_f^{IHClO_4}} + \frac{(C_I)_t}{R + 1}\right] \quad (9f)$$

The last result is identical to eq. 7e when $1/K_f^{IHClO_4} \gg (C_I)_t/(R + 1)$.

The experimental results obtained using 3.78×10^{-6} M PNB with sodium perchlorate (0.013 to 0.11 M) and diethylanilinium perchlorate (0.023 to 0.18 M) in the absence of free base are given in Table IV. The calculated values of R listed in this table were obtained using eq. 9f, $\log K_f^{IHClO_4} = 5.00$,[2a] $\log K_f^{NaClO_4} = 8.38$ and $\log K_f^{BHClO_4} = 9.78$ where B represents diethylaniline. The value 9.78 was used for the logarithm of the formation constant (K_f) of diethylanilinium perchlorate instead of 9.58 as calculated with eq. 4c because it gave better agreement with experiment. This procedure is justified since the uncertainty in the calculated value, 9.58, is sufficiently large to include the value 9.78. The experimental results agree satisfactorily with the calculated values.

TABLE IV

RATIO OF ACID TO BASE FORMS OF p-NAPHTHOLBENZEIN IN SOLUTIONS OF DIETHYLANILINIUM AND SODIUM PERCHLORATE

Cation	Perchlorate, M	Acetate, $M \times 10^5$	$[IHClO_4]/[I]$ Obsd.	Calcd.
Sodium	0.0132	0.00	0.46	0.67
	.0272	.00	.71	.98
	.0537	.00	1.1	1.4
	.108	.00	1.8[a]	2.0
	.108	2.20	1.3	1.2
	.108	4.40	0.94	0.83
	.108	8.80	.60	.48
	.108	17.6	.35	.25
	.108	34.9	.19	.13
Diethylanilinium	0.0226	0.00	0.15	0.17
	.0444	.00	.23	.24
	.0902	.00	.39	.34
	.173	.00	.61	.48

[a] Average of 3 experiments.

The effect of sodium acetate (2.2 to 34.9 $\times 10^{-5}$ M) on 0.108 M sodium perchlorate solution is also shown in Table IV. The calculated values of R were obtained using eq. 9e and the agreement between experiment and predicted values is satisfactory. The data in Table IV indicate that in the titration of 0.1 M sodium acetate with perchloric acid (no volume change) the ratio of the acid to basic form of PNB changes from 0.5 at 0.1% before to 1.8 at the equivalence point. This is a reasonably sharp color change, but of several orders of magnitude smaller than is observed in the titration of a strong 0.1 M base with a strong acid in water.

MINNEAPOLIS, MINNESOTA

[CONTRIBUTION FROM THE REFINING TECHNICAL AND RESEARCH DIVISIONS, HUMBLE OIL AND REFINING COMPANY]

Polarography of Metallic Monolayers

BY M. M. NICHOLSON

RECEIVED AUGUST 6, 1956

The current due to electrolytic dissolution of a thin film in a linear voltage scanning process depends on the changing activity of the solid phase. Starting with Fick's second law of diffusion and an unabridged form of the Nernst equation, a system is derived for calculating the polarographic dissolution curve of a fractional metallic monolayer. Comparison is made with the behavior of a bulk metal deposit. Agreement with experimental data is good for silver, fair for lead and poor for copper, on a platinum electrode. The principles developed here should be useful in analytical applications of film polarography and in the study of electrodeposition phenomena.

The electrochemistry of fractional monolayers has been a subject of interest for many years but is not very well developed. Herzfeld[1] first pointed out that the Nernst equation in its classical form cannot be applied in such cases because it fails to consider variations in the activity of the solid phase. The complexity of surface phenomena which influence electrochemical behavior in the monolayer region is evident in discussions by Haissinsky[2,3] and in a recent review by Rogers.[4] Both of these authors have studied the problem by electrodeposition of radioactive elements from extremely dilute solutions. Although the role of active spots sometimes appears to predominate,[5] it is possible in other instances to interpret results in terms of a relatively uniform deposit, using modifications of the Nernst equation.[6]

The anodic dissolution of a metal film is examined here on the hypothesis of a statistically uniform surface layer, in which the activity is proportional to the fraction of the electrode covered. Experimentally, the dissolution current of an elec-

(1) K. F. Herzfeld, *Physik. Z.*, **13**, 29 (1913).

(2) M. Haissinsky, "Électrochimie des Substances Radioactives et des Solutions Extrêmement Diluées," Hermann, Paris, 1946.

(3) M. Haissinsky, *Experientia*, **8**, 125 (1952).

(4) L. B. Rogers, *Record Chem. Progr.*, **16**, 197 (1955).

(5) M. Haissinsky and A. Coche, *J. Chem. Soc.*, S397 (1949).

(6) L. B. Rogers and A. F. Stehney, *J. Electrochem. Soc.*, **95**, 25 (1949).

trodeposited metal is observed in a linear, polarographic type of voltage scanning process. The current–voltage curve exhibits a characteristic maximum, and the area under the peak is coulometrically equivalent to the amount of metal dissolving. This technique has been applied for trace analytical purposes to silver deposited on platinum[7] and, with some variations, to cadmium,[8] zinc[8] and lead[9] on mercury-plated platinum. The theoretical development in the following section leads to a system for predicting the shape of the dissolution polarogram. Comparisons are made with experimental data for silver, lead and copper films on a platinum electrode.

Theory

Dissolution of a Fractional Monolayer.—Consider the anodic dissolution of a metal M into an unstirred solution containing an excess of supporting electrolyte, and suppose that this metal is in the form of an incomplete monolayer on a planar inert electrode.

$$M \rightleftharpoons M^{n+} + n(-)$$

If the reaction is reversible, a plausible expression for the electrode potential is the unabridged Nernst equation in the form

$$E = E_S + (RT/nF) \ln (\gamma c/a) \quad (1)$$

where E_S is a standard potential, in general not equal to E^0 for the bulk metal, c is the concentration of M^{n+}, γ, its activity coefficient, and a is the activity of the metal M, given by

$$a = m/m_S \quad (2)$$

m represents the number of gram-atoms of M on the surface, m_S, the number at unit activity.

In a linear voltage scan

$$E = E_i + \alpha t \quad (3)$$

E_i is the initial voltage, α is the scanning rate and t is time. The problem is simplified if the concentration is uniform at the beginning of the scan and E_i is chosen to be the equilibrium potential corresponding to the initial values c^0 and a^0. Under these conditions the concentration at the surface is

$$c(0,t) = c^0(a/a^0)\exp(\beta t) \quad (4)$$

where $\beta = \alpha nF/RT$.

The activity a will vary with time according to

$$da/dt = (1/m_S)dm/dt = (AD/m_S)(\partial c/\partial x)_{x=0} \quad (5)$$

in which A is the projected area of the electrode (unless t is extremely small), D is the diffusion coefficient of M^{n+}, and x is distance from the surface.

Diffusion of M^{n+} away from the electrode is governed by Fick's second law.

$$\partial c/\partial t = D(\partial^2 c//\partial x^2) \quad (6)$$

Application of the Laplace transformation to eq. 4, 5 and 6, with conditions 7 and 8

$$c(x,0) = c^0 \quad (7)$$

$$\lim_{x \to \infty} c(x,t) = c^0 \quad (8)$$

results in the equation

$$(c^0/a^0)\bar{a}(s - \beta) - c^0/s + [m_S/(A\sqrt{Ds})][s\bar{a}(s) - a^0] = 0 \quad (9)$$

which has the inverse transform

$$(c^0/a^0)a(t)\exp(\beta t) - c^0 + [m_S/(A\sqrt{\pi D})]\int_0^t (t - \tau)^{-1/2}a'(\tau)d\tau = 0 \quad (10)$$

with $a'(\tau) = da(\tau)/d\tau$. Equation 10 expresses the activity $a(t)$ implicitly in terms of several experimental variables. Further development is facilitated by substitutions 11–14.

$$y = \beta t \quad (11)$$

$$z = \beta\tau \quad (12)$$

$$\psi(y) = a/a^0 \quad (13)$$

$$H = (m^0/Ac^0)(\beta/\pi D)^{1/2} \quad (14)$$

Equation 10 then becomes, after integration by parts

$$\psi(y) = e^{-y} + He^{-y}y^{1/2} + (1/2)He^{-y}\int_0^y (y - z)^{-3/2}\psi(z)dz \quad (15)$$

in which all of the symbols represent dimensionless quantities.

The current is proportional to the flux at the electrode surface

$$i = nFAD(\partial c)/\partial x)_{x=0} \quad (16)$$

and is related to the applied voltage through

$$i = nFm^0\beta\psi'(\beta t) \quad (17)$$

by virtue of 5, 11 and 13. Because

$$q^0 = \int_0^\infty |i|\,dt = nFm^0 \quad (18)$$

17 is equivalent to

$$i/q^0 = \beta\psi'(\beta t) \quad (19)$$

Once the function $\psi'(\beta t)$ has been determined, eq. 19 provides a general system for predicting the current–voltage curves from q^0, β and the dimensionless experimental parameter H. Since

$$-\int_0^\infty \psi'(\beta t)d(\beta t) = 1 \quad (20)$$

a plot of $\psi'(\beta t)$ *vs.* βt is a suitable form in which to compare the shapes of the curves.

Expression 15 is a Volterra integral equation of the general form

$$\psi(y) = f(y) - g(y)\int_0^y K(y,z)\psi(z)dz \quad (21)$$

where $f(y)$, $g(y)$ and $K(y,z)$ are known functions. Numerical solutions for $\psi(y)$ were obtained by the method of Wagner.[10] In this procedure, the distance from zero to y is divided into n small intervals of width h, and within each two consecutive intervals the unknown function is approximated by a quadratic expression. Point by point, values of $\psi(y)$ are calculated throughout the range of interest by application of the recurrence formula

$$\psi(nh) = \frac{f(nh) - g(nh)\sum_{\mu=1}^{n} A_\mu\psi(nh - \mu h)}{1 + g(nh)A_0} \quad (22)$$

where μ is a serial number, and the A's are constants to be determined from a group of special formulas.

(7) S. S. Lord, Jr., R. C. O'Neill and L. B. Rogers, *Anal. Chem.*, **24**, 209 (1952).

(8) K. W. Gardiner and L. B. Rogers, *ibid.*, **25**, 1393 (1953).

(9) T. L. Marple and L. B. Rogers, *Anal. Chim. Acta*, **11**, 574 (1954).

(10) C. Wagner, *J. Math. Phys.*, **32**, 289 (1954).

TABLE I

NUMERICAL DATA AT SELECTED ψ'/ψ'_{max} RATIOS

H →	0.1		1		3		10		100		1000		10,000	
$(-\psi')_{max}$ →	0.709		0.450_9		0.369_2		0.324_8		0.300_0		0.296_4		0.296_0	
ψ'/ψ'_{max}	βt													
1.00	0.23		0.99		1.79		2.87		5.12		7.42		9.72	
0.99	0.16	0.29	0.86	1.12	1.64	1.94	2.70	3.03	4.96	5.29	7.25	7.59	9.56	9.88
.95	.11	.38	.71	1.29	1.44	2.14	2.48	3.23	4.73	5.50	7.03	7.79	9.32	10.09
.90	..	.47	.60	1.43	1.29	2.29	2.31	3.39	4.56	5.66	6.85	7.95	9.15	10.25
.80	..	.63	.45	1.65	1.06	2.52	2.06	3.62	4.28	5.89	6.58	8.19	8.88	10.49
.70	..	.78	.33	1.85	0.87	2.72	1.83	3.83	4.04	6.10	6.33	8.39	8.64	10.70
.60	..	.96	.24	2.04	.71	2.91	1.60	4.03	3.80	6.29	6.09	8.59	8.39	10.90
.50	..	1.15	.17	2.24	.55	3.11	1.38	4.23	3.55	6.49	5.83	8.78	8.13	11.09
.40	..	1.37	.11	2.47	.39	3.34	1.13	4.45	3.26	6.70	5.54	9.00	7.84	11.31
.30	..	1.66	.07	2.73	.25	3.59	0.87	4.71	2.92	6.96	5.20	9.26	7.50	11.57
.20	..	2.05	.04	3.11	.12	3.95	.55	5.05	2.48	7.30	4.75	9.60	7.04	11.90
.10	..	2.84	.02	3.72	.04	4.54	.21	5.62	1.78	7.87	4.01	10.16	6.30	12.47
.05	.00	3.44	.00	4.35	.02	5.13	.06	6.19	1.14	8.43	3.29	10.73	5.58	13.03
.01	.00	4.93	.00	5.86	.00	6.60	.00	7.57	0.20	9.80	1.75	12.08	4.00	14.39

These calculations were performed on an I.B.M. Model 650 Computer for seven values of the parameter H, ranging from 0.1 to 10,000, with $h = 0.1$ in each case. Evaluation of the derivative function $\psi'(y)$ at each n when $y \geq 1$ was included within the sequence of machine operations. For this purpose the mid-range formula of Rutledge[11] was employed

$$\psi'_k = \frac{1}{12\delta}[\psi_{k-2} - \psi_{k+2} - 8(\psi_{k-1} - \psi_{k+1})] \quad (23)$$

In 23, the interval δ was 0.5. The alternate formula

$$\psi'_k = \frac{1}{12\delta}[\psi_{k+3} - 6\psi_{k+2} + 18\psi_{k+1} - 10\psi_k - 3\psi_{k-1}] \quad (24)$$

was applied, with $\delta = 0.2$ for $1 > y > 0.1$, and $\delta = 0.1$ for $y = 0.1$. A comparison run with $h = 0.05$, at $H = 10$, confirmed the ψ values to four significant figures, the ψ' to three, essentially. The maxima were located graphically. Three of the solutions and the corresponding derivatives are shown in Fig. 1. Table I summarizes the numerical results. From this compilation, large plots of $|\psi'|_{max}$ *vs.* log H and βt *vs.* log H at each ψ'/ψ'_{max} ratio were constructed, so that interpolations could be made at any desired value of H.

Certain simplifications occur in the range $H \geq 100$. Here, the peak current is determined by

$$[-\psi'(\beta t)]_{max} = 0.298 \pm 0.002 \quad (25)$$

and as H increases, the ψ' curve shifts along the βt axis according to

$$(\beta t)_2 - (\beta t)_1 = (2.30 \pm 0.01) \log (H_2/H_1) = \ln (H_2/H_1) \quad \text{at constant } \psi'/\psi'_{max} \quad (26)$$

Equation 26 is valid at all ψ'/ψ'_{max} ratios except $\psi'/\psi'_{max} < 0.10$ on the ascending side of the curve. A monolayer dissolving into an extremely dilute solution satisfies the condition for 25 and 26.

Dissolution of a Bulk Metal.—It is interesting to compare the behavior of a fractional monolayer with that of a hypothetical bulk metal film. A dissolution curve for the bulk metal was derived by adaptation of an equation given by Berzins and Delahay[12] for the reverse process of electrodeposition onto a planar surface. Replacing θ in their equation by $-\beta$ yields the dissolution current

$$i = -nFAc^0(\beta D)^{1/2}G(\beta t) \quad (27)$$

where $G(\beta t) = \exp(\beta t)\ \mathrm{erf}[(\beta t)^{1/2}]$. It is assumed that the metal has unit activity until sudden depletion of the film occurs at a time t_{max}. Integration of 27 gives q^0.

$$q^0 = nFAc^0(D/\beta)^{1/2}[G(\beta t)_{max} - (2/\sqrt{\pi})(\beta t)_{max}^{1/2}] \quad (28)$$

The function $i/\beta q^0$ from 27 and 28 appears in Fig. 5.

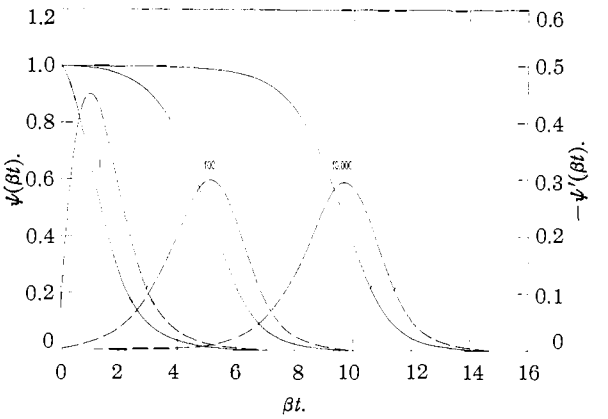

Fig. 1.—$\psi(\beta t)$ and $-\psi'(\beta t)$ at three values of H: —, ψ; — — —, $-\psi'$.

Experimental

Materials.—The water was obtained from a Pyrex conductance water still, and the nitrogen was passed over copper at 450°. Other reagent grade chemicals were used without further purification.

Cell and Electrodes.—A polarographic cell of conventional "H" design was connected to a large saturated calomel electrode through an agar salt bridge, 36 cm. × 0.8 cm.², prepared from a saturated potassium nitrate solution. The polarized electrode was a vertical platinum wire of 0.0255 cm. radius, 0.90 cm. exposed length, 0.144 cm.² geometric area. A glass bead was sealed onto the lower end to minimize edge effects. The cell resistance was 360 ohms with 0.1 M HNO_3 supporting electrolyte, 530 with 0.1 M KCl, and 550 with 0.1 M KNO_3.

High Speed Polarograph.—A high speed recording polarograph was designed and constructed for use with stationary electrodes. Voltage scanning rates up to 50 mv./sec. are provided by a motor-driven Leeds and Northrup No. 4258 Kohlrausch slidewire having ten turns without

(11) G. Rutledge, *Phys. Rev.*, **40**, 262 (1932).

(12) T. Berzins and P. Delahay, THIS JOURNAL, **75**, 555 (1953).

convolutions. Polarograms are recorded on a Brown Potentiometer, 2.5 mv. full-scale sensitivity, 1 sec. full-scale pen response time. The chart speed was $^1/_3$ in./sec. in the present work. The instrument has an adjustable current sensitivity, an independent circuit for setting the initial voltage, and an automatic cell resistance compensator,[13] which is essential in a detailed study of the current-voltage curves.

Procedure.—All measurements were made at 25.0 ± 0.1°, with the cell immersed in a water-bath. During the short intervals when the absence of stirring was required, the temperature control equipment was turned off. The platinum electrode was cleaned in 1:1 nitric acid. Oxygen was removed from the sample compartment by the passage of water-saturated nitrogen.

The electrodeposition step was carried out in a stationary or stirred solution, depending on the amount of metal desired, and the time of plating varied from about 10 sec. to 10 min. Ordinarily, the plating potential was 0.00 v. or −0.10 v. *vs.* S.C.E. for silver, −0.575 for lead, and −0.25 for copper, but less cathodic values were used in some instances to obtain small deposits.

In order to conform to the initial conditions specified in the theory, a stepwise voltage scanning procedure was devised. The anodic scan from the plating potential was interrupted at a point which, by trial, was found to yield zero current after the concentration gradient was destroyed by bubbling with nitrogen for about 20 sec. From this point, E_i, the scan was then continued without stirring, the current-time integral of the last step being q^0. Background currents under the peaks were drawn by inspection, and the dissolution areas were measured with a planimeter. On each new sample, several preliminary plating and dissolution cycles served to remove trace contaminants from the electrode and establish reproducible behavior.

Results and Discussion

The experimental data are recorded in Table II.

TABLE II
EXPERIMENTAL DATA

c^0, moles × cm.$^{-3}$	q^0, μcoulombs	β, sec.$^{-1}$	E_i, volts *vs.* S.C.E.	$-i_{max}$, μamperes	H	$(\beta t)_{max}$	$(-\psi')_{max}$
Silver nitrate in 0.1 *M* nitric acid							
2 × 10^{-9}	38.6	0.649	0.213	7.87	162	5.1	0.298
2 × 10^{-9}	39.7	.649	.213	8.07	166	5.3	.297
2 × 10^{-9}	35.6	.324	.199	3.60	105	5.2	.312
1 × 10^{-7}	49.0	.685	.314	14.1	4.06	2.1	.421
1 × 10^{-7}	39.3	1.297	.314	18.4	4.60	2.4	.362
1 × 10^{-7}	50.3	0.324	.310	7.97	2.94	1.9	.488
2 × 10^{-7}	39.8	.649	.324	15.2	1.65	1.4	.559
2 × 10^{-7}	35.3	.324	.327	8.95	1.03	1.0	.782
2 × 10^{-7}	40.0	.324	.323	9.82	1.17	1.3	.758
2 × 10^{-7}	26.0	1.297	.328	17.2	1.52	1.2	.511
2 × 10^{-7}	213[a]	0.649	.320	84.8	8.83	3.0	.580
Lead nitrate in 0.1 *M* potassium chloride							
1 × 10^{-8}	27.8	0.649	−0.534	7.60	14.5	3.5	0.421
1 × 10^{-8}	6.87	.649	− .533	2.40	3.6	2.3	.538
1 × 10^{-8}	7.40	.649	− .533	2.46	3.8	2.3	.512
1 × 10^{-8}	23.8	1.297	− .535	14.4	17.5	3.9	.466
1 × 10^{-7}	13.4	0.649	− .502	7.90	0.70	1.2	.91
1 × 10^{-7}	9.9	0.649	− .503	6.12	0.52	1.2	.95
Cupric nitrate in 0.1 *M* potassium nitrate							
1 × 10^{-9}	48.7	1.297	−0.076	11.1	400	8.7	0.176
1 × 10^{-9}	48.1	1.297	− .080	11.5	400	8.8	.184
1 × 10^{-9}	62.0	2.595	− .075	24.5	730	10.3	.152
5 × 10^{-8}	34.6	1.297	− .028	8.78	5.6	5.2	.196
5 × 10^{-8}	36.6	1.297	− .031	8.72	6.0	6.3	.184
5 × 10^{-8}	45.5	1.297	− .023	11.4	7.4	4.4	.193
1 × 10^{-7}	82.9	1.297	− .010	17.4	6.8	5.4	.162

[a] Figure 5.

Residual currents have been subtracted and, in the calculation of H, the nominal concentrations were

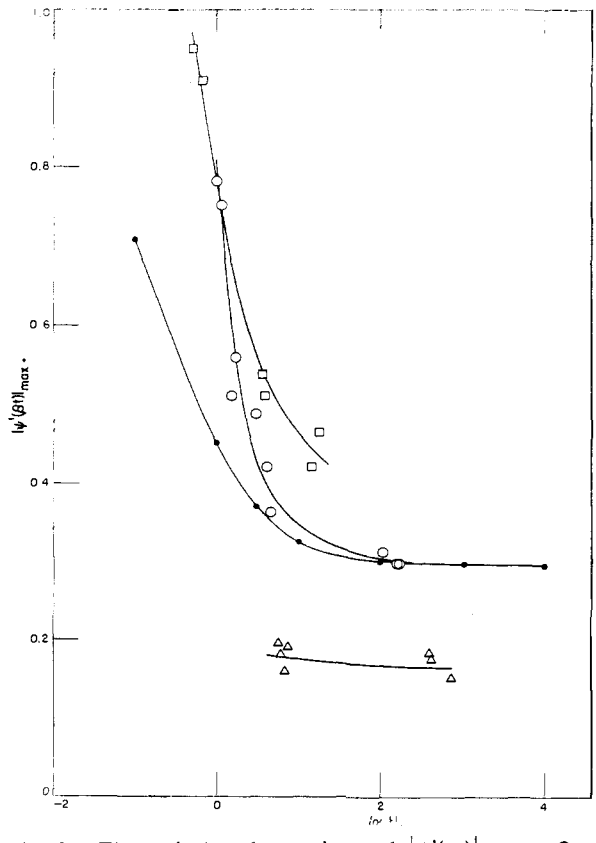

Fig. 2.—Theoretical and experimental $|\psi'(\beta t)|_{max}$: —●—, theory; –O–, silver; –□–, lead; –△–, copper.

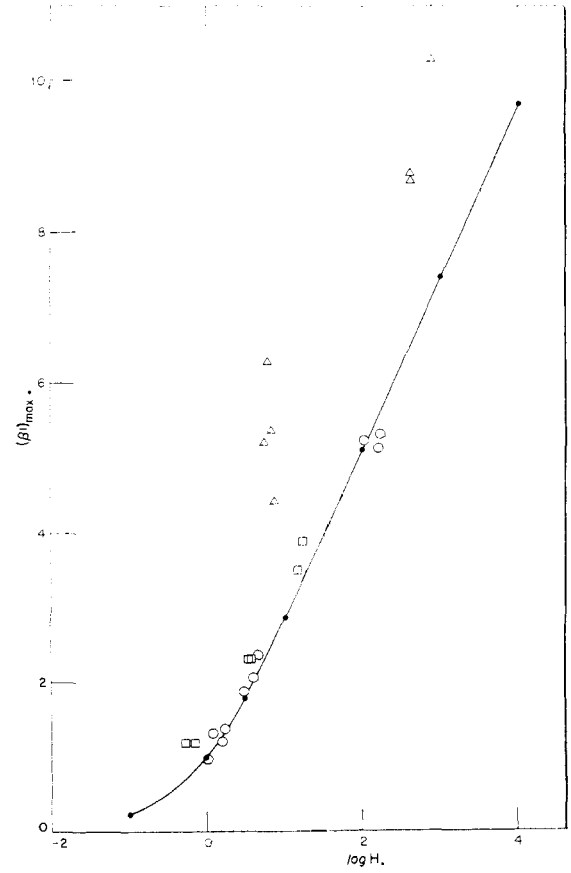

Fig. 3.—Theoretical and experimental $(\beta t)_{max}$: –●–, theory; –O–, silver; –□–, lead; –△–, copper.

(13) M. M. Nicholson, *Anal. Chem.*, **27**, 1364 (1955).

corrected for any significant decreases due to electrodeposition. For silver,[14] $D = 1.553 \times 10^{-5}$ cm.^{2} sec.$^{-1}$; for lead,[15] 0.98×10^{-5}; for copper,[16] 0.80×10^{-5}. Although the concentrations of $PbCl^+$ and Pb^{++} in a 0.1 M chloride solution are of the same order of magnitude,[17] polarographic measurements with the dropping mercury electrode indicate that the diffusion coefficients of the two species are equal within about 5%. Then if the ionic equilibrium is attained rapidly, the total lead content may be represented as a single species in the diffusion problem. Boundary eq. 1 now takes the form

$$E = E'_S + (RT/nF) \ln (\gamma_{Pb^{++}} c/a) \quad (29)$$

where

$$c = c_{Pb^{++}} + c_{PbCl^+} \quad (30)$$

and E_S' is related to E_S for the simple ion by

$$E_S' = E_S + (RT/nF) \ln [K'/(1 + K')] \quad (31)$$

with

$$K' = (K/c_{Cl^-}) (\gamma_{PbCl^+}/\gamma_{Pb^{++}}\gamma_{Cl^-}) \quad (32)$$

K being the dissociation constant of $PbCl^+$.

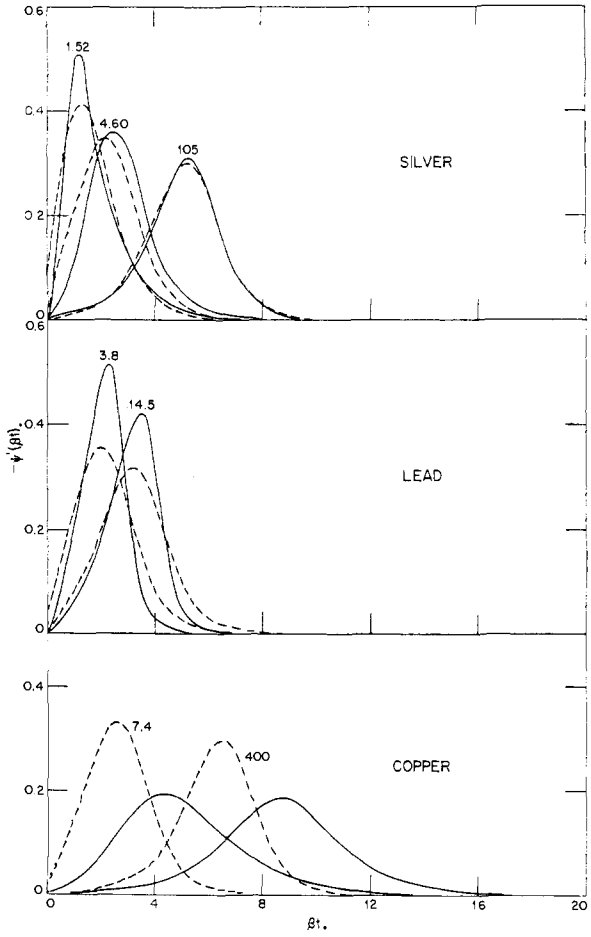

Fig. 4.—Dissolution curves of silver, lead and copper: —, experimental; – – –, theoretical; values of H are indicated.

From the atomic radius and the projected area of the electrode, the minimum electrical equivalent of a complete monolayer can be estimated. Assuming a square lattice on the surface of the 0.144 cm.^{2} electrode, this minimum value is 28 microcoulombs for silver, 38 for lead, and 71 for copper. On this basis, if the roughness factor of the platinum is as great as 1.8, none of the deposits exceeds a monolayer quantity, with the exception of the silver film of 213 microcoulombs.

The present theory does not attempt to predict the initial potential E_i, since E_S would be expected to vary with the nature of the "inert" electrode. It is indeed possible that E_i does not represent a true equilibrium value, in that a redistribution of atoms might occur with prolonged aging of the deposit. "Undervoltages" up to 0.4 volt have been observed for deposition of traces of silver on platinum.[18] However, Rogers and Haissinsky both recognize that adsorption of the metal ion can cause difficulty in the measurement of electrodeposition by the tracer technique. In Table II, none of the E_i values is very different from the bulk metal potential calculated by the classical Nernst equation. Averages of $E_{bulk} - E_i$ are +0.002 v. for silver, −0.009 for lead, with K = 0.03, and −0.024 for copper.

Theoretical and experimental values of $\psi'(\beta t)$ at the maximum currents are shown in Fig. 2. At large H, the silver points merge with the theoretical

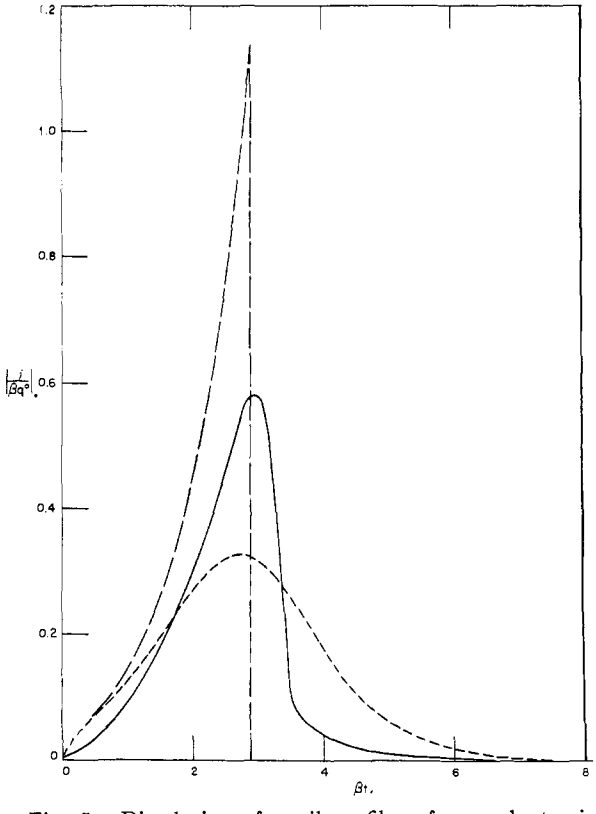

Fig. 5.—Dissolution of a silver film of several atomic layers: —, experimental, 213 μcoulombs; – – –, monolayer theory, H = 8.83; — —, bulk metal theory, 213 μcoulombs.

(14) M. von Stackelberg, M. Pilgram and V. Toome, *Z. Elektrochem.*, **57**, 342 (1953).

(15) I. M. Kolthoff and J. J. Lingane, "Polarography," 2nd Edition, Interscience Publishers, New York, N. Y., 1952, p. 529.

(16) R. B. Dean, THIS JOURNAL, **67**, 31 (1945).

(17) R. M. Garrels and F. T. Gucker, *Chem. Revs.*, **44**, 117 (1949).

(18) J. T. Byrne, L. B. Rogers and J. C. Griess, Jr., *J. Electrochem. Soc.*, **98**, 452 (1951).

curve. The deviation at small H may be due to curvature of the electrode surface, which would have a more pronounced effect as β decreases. The data for lead lie on a different curve of the same general shape, while copper falls far below the calculated line, even at large H. This behavior of the three metals is reflected in terms of the peak potentials in Fig. 3. On the βt scale, 0.1 unit is equivalent to 2.5 mv. for a one-electron process. More detailed comparisons are provided by the complete $\psi'(\beta t)$ curves of Fig. 4. With silver, at $H = 105$, the agreement is remarkably good in all details, and the predicted trends in shape are retained as H diminishes. The deviations of lead and copper appear to be caused by different phenomena.

The contrast between bulk metal films and fractional monolayers is depicted by Fig. 5, which includes the dissolution curve of the silver film with $q^0 = 213$ microcoulombs. The conditions of this measurement, corresponding formally to $H = 8.83$, would give relatively good agreement in the case of a monolayer, according to Fig. 2. The actual film probably has a thickness of several atomic layers, and its transitional character is evident from the shape of the curve.

Any conclusions regarding the distribution of atoms on the surface must be drawn with caution, since the problem doubtless is complicated by many factors not included in the theory presented here. It can be observed, however, that the dissolution patterns of thin silver films are consistent with the assumption of a uniform monolayer, that the curves of lead show some tendency toward macro behavior, even at the lower surface coverages, which may indicate preferential deposition on like atoms, and that the forms of the anodic copper polarograms suggest the possibility of a slow step in the reaction mechanism. Byrne and Rogers[19] eventually concluded that silver atoms deposit first as a monolayer on platinum but probably with a heterogeneous distribution of energies. Haissinsky and Coche[5] arrived at approximately the same result for lead on platinum. Comparable data apparently are not available on the copper-platinum system. Hillson[20] in a study of the copper–cupric ion couple by alternating current electrolysis, reported that the exchange reaction on the bulk metal is rapid but occurs only on a small fraction of the electrode area. Duncan and Oakley[21] found an unexpectedly low rate of isotopic exchange between cupric ion and an oxide-free copper surface.

Although the monolayer theory was derived from a simplified model, it establishes the importance of certain parameters and provides a framework for comparison of results on various chemical systems. Thus it should be helpful in development of analytical methods and in the study of electrodeposition phenomena.

Acknowledgments.—The writer is greatly indebted to Mr. R. E. Tannich for development of the program for machine calculations and to Mr. Carl P. Tyler for aid with the experimental work.

(19) J. T. Byrne and L. B. Rogers, *J. Electrochem. Soc.*, **98**, 457 (1951).

(20) P. J. Hillson, *Trans. Faraday Soc.*, **50**, 385 (1954).

(21) J. F. Duncan and B. W. Oakley, *J. Chem. Soc.*, 1401 (1955).

BAYTOWN, TEXAS

[CONTRIBUTION FROM THE DEPARTMENT OF CHEMISTRY, MASSACHUSETTS INSTITUTE OF TECHNOLOGY]

Physical Chemistry of Protein Solutions. VII. The Binding of Some Small Anions to Serum Albumin[1]

BY GEORGE SCATCHARD, JAMES S. COLEMAN AND AMY L. SHEN

RECEIVED JULY 31, 1956

A cell is described for the measurement of the change in electromotive force with a change in the concentration or composition of a solution between an anion and a cation exchanger membrane, or between either membrane and a saturated potassium chloride bridge. Measurements are reported for the case of adding bovine serum mercaptalbumin to solutions of sodium chloride, sodium iodide, sodium thiocyanate, sodium trichloroacetate, hydrochloric acid, hydriodic acid, thiocyanic acid or to mixtures of sodium chloride with hydrochloric or with sodium hydroxide. The binding of an anion to the albumin is calculated from the measurements with the neutral salt, and the effect on pH agrees with simple electrostatic theory. This binding corresponds to three groups of sites on the albumin with the ratio of the constants for each group 3.85 for I^-/Cl^- and 19.25 for SCN^-/Cl^- and $Cl_3CCO_2^-/Cl^-$. The first group contains a single site, the second 8 sites and the third 18 sites. The chloride constants are $K_{1Cl} = 2400$, $K_{2Cl} = 100$ and $K_{3Cl} = 3.3$. There are about 70 other groups with smaller constants. The measurements in acid solutions indicate that the affinity for anions becomes smaller than that calculated from simple theory as the affinity for protons becomes larger, though not to the same extent. The changes appear to depend upon the number of protons bound rather than upon the charge.

Introduction

Ion exchangers have advantages in the electrochemical study of protein solutions because their pores are too small to admit protein molecules and because they repel ions of the same sign. Therefore, even in the presence of protein, a cation exchanger membrane behaves as a small-cation electrode and an anion exchanger membrane as a small-anion electrode in the same sense that a glass membrane may behave as a hydrogen electrode.

Some advantages are that there is no oxidation or reduction at these membranes, they are not limited to ions for which there are reversible true electrodes, and the combination of a cation and an anion exchanger permits the measurement of the free energy of transfer of the salt.

We have not used the last two advantages to the utmost in this work because we wished to study

(1) Adapted in large part from the Ph.D. Thesis of James S. Coleman, M.I.T., 1953.